Available online at www.sciencedirect.com
ScienceDirect
Experimental Thermal and Fluid Science xxx (2007) xxx–xxx
Experimental Thermal and Fluid Science
www.elsevier.com/locate/etfs

Wall skin friction and mean velocity profiles of fully developed turbulent pipe flows

E.-S. Zanoun [a,*], F. Durst [b], O. Bayoumy [b], A. Al-Salaymeh [c]

[a] Department of Aerodynamics and Fluid Mechanics (LAS), BTU Cottbus, Siemens-Halske-Ring 14, D-03046 Cottbus, Germany
[b] Institute of Fluid Mechanics (LSTM-Erlangen), Friedrich-Alexander-University, Cauerstr. 4, D-91058 Erlangen, Germany
[c] Mechanical Engineering Department, Faculty of Engineering and Technology, University of Jordan, Amman 11942, Jordan

Received 20 April 2006; received in revised form 20 November 2006; accepted 4 April 2007

Abstract

The friction factor $\lambda(Re)$ and the mean velocity $U^+ = f(y^+)$ measurements of Nikuradse [J. Nikuradse, Gesetzmässigkeiten der turbulenten Strömung in glatten Rohren, Forschg. Arb. Ing.-Wes. No. 356 (1932); J. Nikuradse, Strömungsgesetze in rauhen Rohren, Forschg. Arb. Ing.-Wes. No. 361 (1933)] of fully developed turbulent flows in smooth and rough pipes are of vital consideration since they provided the data by which established theories have been developed in the last few decades. The pressure gradient and the resultant friction factor of Nikuradse' smooth pipe agree well with the authors' own results. On the other hand, the Nikuradse's corresponding mean velocity profile measurements show differences from measurements presented in this. The differences might be attributed to the state of Nikuradse's flow at the location of velocity profile measurements in addition to differences in the applied measuring techniques. It is concluded that pitot tubes do usually not have the needed spatial resolution in the near-wall region and produces therefore velocity overshoots under $y^+ = 300$ when used in turbulent pipe shear flows. Hence, when the lower limit for the log-range starts at $y^+ \leqslant 50$, which was common for almost all previous work up to the late 1990s, a higher value for the so-called von Kármán constant (κ) of the logarithmic velocity profile resulted. In addition to pitot tube velocity measurements, hot-wire measurements are provided, showing that the slope (i.e., $1/\kappa$) of the logarithmic velocity profile is inconsistent with value deduced from the $\lambda(Re)$ measurements performed by the authors. Nikuradse's pitot tube velocity data also yield log law constants that are not reflected by their corresponding pipe friction measurements. However, the authors observed that the hot wire and pitot tube results are about the same if the inner limit of the log range of the logarithmic velocity profile is $y^+ \geqslant 300$ and the effect of the mean shear gradient is minimal under the same condition.

Keywords: Pipe flow; Logarithmic velocity profile; Friction factor

1. Introduction and aim of work

It is occasionally claimed that the data published by Nikuradse for turbulent smooth pipe [19] and turbulent rough pipe [20] flows are somewhat inconsistent (see, e.g., Hinze [14], and Zagarola and Smits [32]). However, seeking more details about this claim, one obtains very little and imprecise information as to where these inconsistencies lie. This is the current situation, although Nikuradse's pipe flow experiments still represent the most extensive study of the mean flow properties of turbulent pipe flows over a wide range of Reynolds numbers. Nikuradse's turbulent pipe flow investigations led the present authors to look more closely at his paper published in 1932 and encouraged them also to investigate turbulent smooth pipe flows further. Nikuradse [19,20] documented impressive investigations into basic turbulent flows, often employed to study turbulence, showing good data for the mean pressure gradient and pitot tube measurements of the mean velocity distributions in pipe flows over a wide range of Reynolds numbers. Data are available from Nikuradse's experiments

* Corresponding author. Tel.: +49 0355695127; fax: +49 0355694545.
E-mail address: ezanoun@netscape.net (E.-S. Zanoun).

0894-1777/$ - see front matter © 2007 Elsevier Inc. All rights reserved.
doi:10.1016/j.expthermflusci.2007.04.002

up to high Reynolds number, $Re \leqslant 3.2 \times 10^6$, and his experimental test rig and the measuring procedures employed were described with care so that one can assess both the performance of his equipment and also the accuracy of his data. In spite of the care taken, the reported mean velocity distributions seem to show inconsistency with respect to the corresponding friction data calculated from the mean pressure gradient measurements, and this is detected when accurate values for the constants of the log law are deduced. One of the major problems with Nikuradse's experiment was his definition of the minimum entrance length (L), needed to assure the state of the fully developed flow before his velocity profiles' measuring station. Nikuradse [19] concluded, by comparing the mean velocity profiles at successive streamwise distances from the pipe inlet, that flow was fully developed between 25 and 40 of pipe diameter (D), which was not enough to assure good mean flow data in all respects. For instance, Abell [1] recommended an entrance length between $71.9D$ and $86.2D$, when flow was tripped at the pipe entrance to obtain a good state of fully developed flow, see also Patel and Head [24]. More recently, Zagarola and Smits [32] found that an entrance length of $160D$, without tripping the flow at the pipe inlet, is needed to assure the fully developed state of turbulence in the pipe flow. Therefore, Nikuradse's short entrance length might be one reason for the claim of the higher values of both the von Kármán constant, κ, and the additive constant, B, in the logarithmic velocity distribution deduced from not fully developed mean velocity measurements. It is also shown in this paper that a discrepancy appeared was caused by the diameter of the pitot tubes that Nikuradse employed, in addition to assumptions used to derive the logarithmic friction relationship by Prandtl [27]. Although the pitot tubes used by Nikuradse were small in absolute size, they were large in terms of wall units, ν/u_τ, especially for the very high Reynolds numbers in his investigations, and the applied corrections are known to not completely eliminate the influence of the pitot tube diameter.

In the present paper, Nikuradse's pipe flow measurements are considered in detail and compared with the present authors' corresponding results. The latter were obtained by means of both pitot tube and hot-wire anemometry. The later method was employed to yield the locality of the mean velocity measurements needed to deduce correctly the von Kármán constant, κ, and the additive constant, B, in the logarithmic velocity profile. The present paper shows that the authors' $U^+(y^+)$-measurements resulted in κ and B values that are not consistent with values deduced from the $\lambda(Re)$ relationship which also embraces Nikuradse's $\lambda(Re)$ results. To prove the cause of Nikuradse's inconsistency in the κ value deduced from the $U^+(y^+)$ and from the friction measurements (i.e., $\lambda(Re)$-data), the present authors repeated some of Nikuradse's pitot tube measurements in their pipe flow test facility. The resultant data showed velocity overshoot, i.e., higher values for the mean velocity in the region close to the pipe wall since the $U^+(y^+)$ values represent mean velocities that are obtained through integrations over the Δy^+ range defined by the normalized pitot tube inlet diameter within the wall shear layer. Using the hot-wire anemometry results, it is shown that the deduction of the log law constants, i.e., κ and B, from the normalized mean velocity can be obtained accurately. However, if points on the velocity profile measurements that do not belong to the region where the logarithmic velocity profile holds are taken into account, the deduced values of both κ and B are wrong. Characteristic functions are used to deduce the region of the velocity profile that is well described by the log law and it is stressed in the paper that only points from this region should be used to derive both constants. This finding and other observations made during the measurements encouraged the authors to suggest a sequence of measurements and data evaluations for investigating fully developed turbulent pipe flows.

In Section 2, a summary of the scaling laws for the mean flow properties of fully developed turbulent pipe flow is given. Section 3 describes the test rig and its functioning and the measuring techniques employed. Section 4 reports the mean pressure gradient and cross-sectional averaged velocity measurements that were used to deduce friction factor data. In Section 4, the mean velocity measurements utilizing the hot-wire anemometry are also reported to yield κ and B in the logarithmic velocity profile. In Section 5, Nikuradse' skin friction data and the corresponding data of the authors are addressed and discussed. Finally, the paper suggests consistency checks of the measured $\lambda(Re)$ distribution and the mean velocity data, showing differences when used to derive information about the constants of the logarithmic velocity profile. Conclusions and final remarks are given in Section 6.

2. Scaling laws for pipe flow

Axisymmetric, fully developed, turbulent pipe flow is one of the most reproducible flows in the laboratory for wall-bounded shear flow investigations. It is also considered to be important in practice owing to its wide applications. Therefore, this classical type of flow has attracted the attention of a large number of researchers. In spite of this fact, the issue of the wall functional relations, at high enough Reynolds numbers, is still a mysterious problem in turbulent pipe flows. To resolve this problem, the exact streamwise mean momentum equation for fully developed pipe flow is considered and written in the following simplified form

$$-\rho\overline{uv} + \mu\frac{\mathrm{d}U}{\mathrm{d}y} = \frac{1}{2}(y-R)\frac{\mathrm{d}P}{\mathrm{d}x}, \tag{1}$$

and the viscous force, $2\pi\rho(u_\tau)^2$, is balanced by the mean pressure force, i.e.

$$2\pi R\rho u_\tau^2 = -\pi R^2\frac{\mathrm{d}P}{\mathrm{d}x}, \tag{2}$$

Please cite this article in press as: E.-S. Zanoun et al., Wall skin friction and mean velocity profiles of fully developed ..., Exp. Therm. Fluid Sci. (2007), doi:10.1016/j.expthermflusci.2007.04.002

results in the mean momentum equation in pipe flow to be rewritten as

$$-\rho\overline{uv}+\mu\frac{\mathrm{d}U}{\mathrm{d}y}=\rho\left(1-\frac{y}{R}\right)u_\tau^2. \tag{3}$$

where R is the pipe radius. This form of the mean momentum equation for two-dimensional pipe flow needs to be supplied with closure assumptions regarding the turbulent momentum transport term $-\rho\overline{uv}$ to be solved for the mean velocity distribution. There are some classical and recent methodologies for modeling $-\rho\overline{uv}$ (see, e.g., Boussinesq [4], Prandtl [25,26], Taylor [29], von Kármán [31], Deissler [9], and Panton [23]) as far as the mean properties of the fully developed turbulent pipe flow are concerned to obtain information about the mean velocity profile, i.e.,

$$\begin{aligned}\frac{\mathrm{d}U^+}{\mathrm{d}y^+}&=\left(1-\frac{y^+}{R^+}\right)-(-\overline{uv}^+)\quad\Rightarrow\quad U^+\\&=\int_0^{R^+}\left[\left(1-\frac{y^+}{R^+}\right)-(-\overline{uv}^+)\right]\mathrm{d}y^+,\end{aligned} \tag{4}$$

where the normalization of all terms in Eq. (4) was carried out with the following characteristic velocity, length and time scales:

$$u_c=u_\tau=\sqrt{\tau_w/\rho},\quad l_c=\nu/u_\tau,\quad t_c=\nu/u_\tau^2. \tag{5}$$

R^+ is called the Kármán number and is defined as $R^+=u_\tau R/\nu$. Considerations suggested that the data to be measured to analyze flow described by Eq. (3) should be either $\mathrm{d}U/\mathrm{d}y$ or $-\rho\overline{uv}$. To measure or model $-\rho\overline{uv}$ in the region where it is the much larger term in Eq. (3) is not the right way for $U(y)$ to be deduced correctly from Eq. (4), since a small error in the $-\rho\overline{uv}$ will yield a large error in the deduced $U(y)$ distribution (see, e.g., Laufer [16] and, more recently, Gad-el-Hak and Bandyopadhyay [12]).

Integrating Eq. (4) results in the logarithmic velocity profile which is usually considered to be valid in the inertial sub-layer where $yu_\tau/\nu\gg1$ and $y/R\ll1$, as proposed by Prandtl [25,26], von Kármán [31] and Millikan [18]:

$$\frac{U}{u_\tau}=\frac{1}{\kappa}\ln\left(\frac{yu_\tau}{\nu}\right)+B, \tag{6}$$

where κ is the von Kármán constant and B is an additive constant. These constants are claimed to be universal. However, a wide scatter around the most accepted values, i.e., $\kappa=0.4$ and $B=5.5$, was found in the literature, see Zanoun et al. [33,34] for more details.

Utilizing the logarithmic velocity profile, i.e., Eq. (6), the bulk flow velocity can be defined as follows:

$$U_\mathrm{b}=\frac{1}{\pi R^2}\int_0^R 2\pi(R-y)U\mathrm{d}y, \tag{7}$$

$$\frac{U_\mathrm{b}}{u_\tau}=\frac{1}{\kappa}\ln\left(\frac{Ru_\tau}{\nu}\right)-\frac{3}{2\kappa}+B. \tag{8}$$

Rearranging Eq. (8) results in the following logarithmic friction relation for flow in pipes:

$$\sqrt{\frac{8}{\lambda}}=\frac{1}{\kappa}\ln\left(Re\sqrt{\frac{\lambda}{32}}\right)-\frac{3}{2\kappa}+B. \tag{9}$$

Based on the smooth wall pipe flow data of Nikuradse [19], Prandtl [27] adapted the constants of Eq. (9) to read as:

$$\sqrt{\frac{1}{\lambda}}=2\log\left(Re\sqrt{\lambda}\right)-0.8, \tag{10}$$

which is known as the universal friction law for hydraulically smooth pipe flows. More details about Eqs. (9) and (10) are presented and discussed in Section 5.

3. Test section and measuring equipment

3.1. Test section

To clarify the inconsistency of the log law constants obtained from Nikuradse's wall friction and mean velocity data in smooth pipe flow, the authors carried out their own pipe flow experiments. The investigations were carried out at LSTM-Erlangen using the pipe test facility shown in Fig. 1. The actual air flow was provided by a centrifugal blower which had a maximum capacity of 10 m^3/s and was powered by a 20 kW motor. The blower outlet was connected to a well-designed settling chamber to ensure the uniformity of the flow entering the pipe test section. After the outlet of the blower, the first essential flow control device was located, consisting of two perforated plates with 52% solidity, having square openings of 10×10 mm^2. The perforated plates were separated in the flow direction by a 30 cm distance from the blower and from each other. The second passive flow control device in the plenum chamber was a flow straightener "honeycomb" with a mesh size of 8 mm diameter and 160 mm total length of the tubes. These passive flow control devices inside the plenum chamber were located in such a way as to yield a well-controlled inlet flow to the pipe test section. The entire flow was setup in accordance with suggestions made by Loehrke and Nagib [17].

The pipe flow rate for each investigated Reynolds number was controlled by changing the speed of the plated rotor of radial blower blades by means of a frequency converter control unit, providing impeller rotational speeds in the range of approximately 100–2000 rpm. These settings corresponded to a mean velocity range of the pipe flow from 2 m/s to 50 m/s with a centerline turbulence level of less than 0.3% at the axis of the pipe inlet cross-section. The authors used a special Venturi flow nozzle at the inlet of the settling chamber for measuring the mean volume flow rate and consequently the bulk flow velocity through the pipe test section for each investigated Re. In addition, the bulk flow velocity was obtained by integrating the velocity profile at the measuring station to ensure a good assessment of the bulk air velocity, U_b, as the time and area averaged velocity for each Re case. Good agreement of about ±1% was achieved for the average velocity from the Venturi nozzle and the bulk air-flow velocity was then

Please cite this article in press as: E.-S. Zanoun et al., Wall skin friction and mean velocity profiles of fully developed ..., Exp. Therm. Fluid Sci. (2007), doi:10.1016/j.expthermflusci.2007.04.002

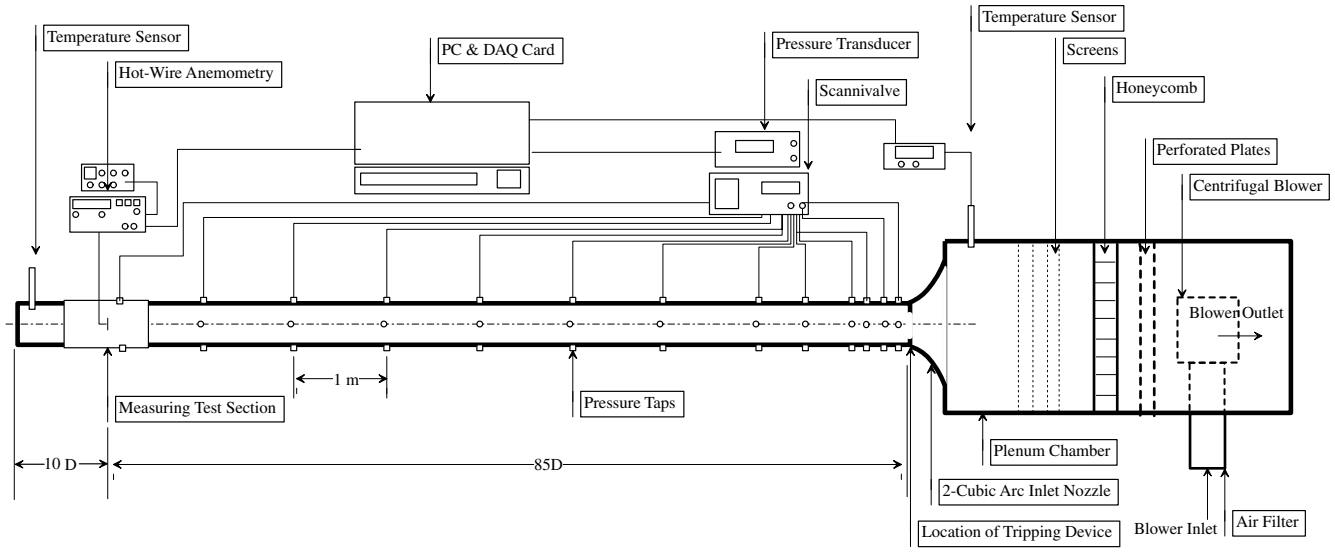

Fig. 1. Sketch of the pipe flow test section showing the temperature, pressure, velocity measuring equipment and tripping device.

used to compute the bulk Reynolds number of the flow, $Re = U_b D/\nu$. A medium range of Reynolds numbers up to $Re \approx 4.5 \times 10^5$ was set up in this way.

The pipe test section was made of a high-precision smooth brass tube with a surface roughness measured accurately to have a mean value of $r_a = \pm 0.25$ μm, which, in terms of wall units, was less than 0.03 for the higher investigated Reynolds number. The pipe was therefore considered to be hydrodynamically smooth at all Reynolds numbers considered. The geometric dimensions of the pipe showed an internal diameter, D, of 148 mm and a length of 14 m, providing $L/D \approx 95$. The pipe consisted of three sections, two with a length of 5 m per each and the third with a length of 4 m, connected together by custom-designed couplings. A schematic diagram of the pipe test section was shown in Fig. 1 where all velocity profiles measurements were taken at $L/D = 85$. A two-cubic arc inlet nozzle to the pipe was made out of hard wood having a circular cross-section and a contraction ratio of 11.4. This nozzle was used between the plenum chamber and the pipe test section to assure a smooth pipe inlet flow. An inlet fence (orifice) was employed at the actual pipe inlet to trigger the turbulence development along the initial test section of the pipe. To study the effect of the inlet fences, different fences were mounted, individually at the pipe entrance, i.e., at $L/D = 0$, with a height of $\delta/D = 10\%$, 20%, 30% and 40% area blockage to trigger the flow over the circumference of the pipe cross-section. This was studied to yield the effect of flow tripping on the friction factor and the mean velocity profiles. However, for the final measurements $\delta/D = 10\%$ was chosen. The height of this tripping fence, i.e., $\delta/D =$ 10%, was found to be enough according to intensive measurements by Fischer [11] to ensure a well-tripped turbulent pipe flow at the measuring location. It was ensured that turbulent flow properties were well reached at the measuring station, i.e., at $L/D = 85$, where all measurements are reported. This was in agreement with Patel and Head [24] who concluded that both the mean and the fluctuating velocity distributions in a turbulent pipe flow indicate a full development state for a downstream distance of 50–80D. This was confirmed in the present measurements and therefore the present measurements were taken at $L/D = 85$.

At each x-location, for pressure measurements in the streamwise direction, three static pressure taps of 400 μm diameter were carefully installed around the circumference of the pipe. The mean static pressure at each x-location was obtained by averaging measurements of the three pressure taps. Away from the pipe entrance, the mean pressure gradient needed for estimating the wall skin friction was obtained from ten different pressure locations, all being 1 m apart from each other (see Fig. 1). The distance of $x/D = 24$ from the inlet was found to be sufficient to ensure full development of flow pressure. Observations, made also by Patel and Head [24], indicated that the mean pressure gradients showed an earlier state of full development at distance between 10 and 20D from the pipe inlet test section. The last location for wall pressure measurements where also the authors' hot-wire and pitot tube measurements were carried out was far enough away from the pipe outlet, i.e., $\Delta x/D = 10$, to ensure that there were no outlet disturbances to the investigated flows. Care was taken also to ensure that the inner surface of the pipe, where the pressure holes were drilled, was free from remaining drilling defects of the holes (i.e., smoothness was insured around the pressure tappings from the inner side of the pipe surface). Hence, as the above description shows, the test facility was designed and built carefully to carry out fully developed turbulent pipe flow measurements over a medium range of Reynolds numbers.

3.2. Measuring techniques

Streamwise mean pressure gradient measurements were carried out to deduce from them the wall shear stress, τ_w,

for each investigated Re of the flow. A precise pressure transducer was employed for pressure measurements at each downstream location having an accuracy of ±0.25% of the actual readings. All pressure measurement points were connected to a scannivalve to facilitate switching from one point to another and the corresponding static pressure was then measured and recorded for the different air flow velocities, corresponding to different Re. Utilizing the results of the pressure measurements and the corresponding air stream temperature in the pipe, both the air density and kinematic viscosity were calculated using the ideal gas relationships and Sutherland's correlation; see Section 4.

Local mean static pressure measurements were employed to evaluate the streamwise pressure gradient, $\mathrm{d}P/\mathrm{d}x$, which in turn was employed to obtain the wall shear stress, τ_w, and then the wall friction velocity, u_τ. As a result, the wall skin friction data were computed, independently of the mean velocity profile measurements, i.e.,

$$\lambda = -\frac{\mathrm{d}P}{\mathrm{d}x}\frac{D}{1/2\rho U_b^2} \quad \text{and}$$
$$\tau_w = -\frac{R}{2}\frac{\mathrm{d}P}{\mathrm{d}x} \Rightarrow \lambda = 8\left(\frac{u_\tau}{U_b}\right)^2, \quad \text{where} \quad u_\tau = \sqrt{\frac{\tau_w}{\rho}}. \qquad (11)$$

Two temperature sensors were used to measure the temperature within an accuracy of ±0.05 °C. One position was close to the pipe inlet, i.e., close to the exit of the settling chamber, and the other was close to the pipe outlet, i.e., $x/D = 2.5$ (see Fig. 1). The ambient conditions were monitored in the laboratory and reported for each test run using an electronic barometric sensor. All electronic equipment were connected to a 16-bit A/D DAQ card having 8 channel inputs. In addition, a computer-based programming system was used for acquiring and processing all the data measured.

The velocity profile measurements were carried out using both a pitot tube and a DANTEC 55M10 constant-temperature anemometer. Hot-wire measurements of the local velocity were made utilizing a boundary layer probe equipped with a 5 μm diameter wire and 1.25 mm an active wire length, providing an aspect ratio, l/d, of 250. Hence the wire had a sufficiently large aspect ratio to suggest a negligible influence of the prongs on the actual velocity measurement. All calibrations and measurements were performed with an 80% overheat ratio, $a = (R_w - R_a)/R_a$, where R_w is the operational hot-wire resistance and R_a is the resistance of the cold wire, i.e., at ambient air temperature. A correction for temperature drift was taken into account for unavoidable temperature changes of the working air during calibrations and measurements, see, e.g., Bearman [3], Bremhorst [5] and Crowell et al. [8]. In the present study, an instantaneous correction for the hot-wire output was carried out for the case that a small, i.e., $\Delta T \leqslant 0.3$ °C, temperature drift existed.

The pitot-probe velocity measurements were made by traversing a total-head probe of 1 mm inner diameter over the pipe cross-section. The pitot probe was designed according to the recommendations of Bryer and Pankhurst [6] and Sami [28]. Among other things, the inner diameter of the pitot probe was chosen to be half of the outer diameter. To obtain the dynamic head for velocity calculation, the pipe wall static pressure was measured at a distance of 6 times pitot diameter in the downstream direction of the pitot tube inlet. The outlet of the pitot tube was then connected to a precision pressure transducer operated via the data acquisition system. Using the incompressible Bernoulli equation, the pitot probe measurements were converted to velocity.

The wall distance measurements were of vital importance in the present work and therefore great care was taken to ensure a precise location of the hot wire and the pitot tube at a reference distance from the wall. To position the hot wire, a calibration positioning procedure proposed by Bhatia et al. [2], and Durst et al. [10] was applied. In addition, the zero position of the pitot probe was specified by measuring the resistance between the pipe wall and the body of the pitot probe. The absolute error in positioning both the hot wire and the pitot probe was found to be less than ±5 μm.

4. Experimental results and discussion

4.1. Pressure measurements and friction factor

The local skin friction is an essential quantity for investigating wall-bounded shear flows to represent data in a normalized form as $U^+(y^+)$ profiles. For instance, precise estimation of the parameters of the logarithmic velocity profile requires accurate values for the wall shear stress measured independently from the mean velocity measurements. In pipe flows, the mean pressure gradient, $\mathrm{d}P/\mathrm{d}x$, measurements provide a simple and accurate method to obtain the wall shear stress, τ_w, which in turn was employed to calculate the wall friction velocity, u_τ, utilizing Eq. (11). In addition to the mean pressure gradient measurements, the bulk flow velocity for each set of measurements was obtained by measuring the dynamic pressure through an inlet nozzle to the settling chamber where a uniform and well-defined flow field existed.

Simultaneously with the mean pressure measurements, and corresponding to the air stream temperature in the pipe test section, the air density and kinematic viscosity were calculated for the purpose of normalization using the following relations for density:

$$\rho = \frac{P_{atm} + P_{st}}{\Re T}, \qquad (12)$$

and the well-known Sutherland's correlation for the kinematic viscosity:

$$\nu = 1.458 \times 10^{-6}\frac{T^{3/2}}{\rho(T + 110.4)}, \qquad (13)$$

where P_{atm} is the atmospheric pressure, P_{st} is the static pressure and $\Re = 279.1$ J/kg K is the specific constant for air employed in the ideal gas law.

Utilizing the mean pressure gradient measurements in connection with the bulk flow velocity, the pipe wall friction data were obtained independently of the velocity profile measurements. However, it is customary to express the flow pressure drop measurements in terms of the friction factor, i.e., in the form of λ versus Re, instead of the wall friction velocity as expressed in Eq. (11). Fig. 2 shows, therefore, a comparison between the present pipe friction data and the data extracted from the literature. Good agreement was observed when the present data were compared with those of Zagarola and Smits [32] and also with Prandtl's relation (i.e., Eq. (10)). It is worth mentioning that the present pipe wall friction data were obtained for different heights of the tripping device employed. The resultant friction factors obtained through these measurements compare well with the data reported by Nikuradse [19], showing that the height of the tripping fence has basically no influence on the pressure and the bulk velocity readings employed to compute the friction factor plotted in Fig. 2. Hence all fully developed measurements of the mean velocity were performed utilizing 10% tripping, see, Fischer [11], for all further investigations using the hot-wire anemometry and the pitot tube.

4.2. Mean velocity profile and log law constants

It is common in the fluid mechanics community to divide the flow field of wall-bounded flows mainly into two different regions, i.e., an inner and a core regions, see, e.g., von Kármán [31] and Prandtl [26]. As a result, a number of proposed velocity distributions can be found in the literature and can be used either in the inner or the core region. Among these laws are the logarithmic law and the power law that can be utilized to represent the mean velocity measurements over part of the pipe cross-sectional area, e.g., in the overlap region. For the logarithmic representation of the mean velocity distribution, the so-called von Kármán–Prandtl universal log law was suggested, taking the following well-known form:

$$U^+ = \frac{1}{\kappa}\ln y^+ + B, \tag{14}$$

where κ and B are assumed to be universal constants, i.e., independent of Re in the limit of infinite or high enough Re.

A Reynolds number-dependent power law is an alternative representation of the mean velocity profile in the overlap region that was proposed by Millikan [18] and more recently by Wosnik et al. [35], written in the following form:

$$U^+ = Cy^{\gamma}, \tag{15}$$

where C and γ are empirically determined parameters, which are often assumed to be Reynolds number dependent; see, e.g., Clauser [7].

Recently, it was observed that the estimation of the log law parameters is sensitive to the log range, i.e., the wall-distance of the data employed for the overlap region. Only from the mean velocity distribution $U = f(y^+)$, it becomes not clear how to directly identify the appropriate log range for the logarithmic velocity profile, see, e.g., Österlund et al. [21], Zanoun et al. [34]. To clarify this point, the mean velocity profiles of Nikuradse [19] scaled with the inner wall variables, u_τ, and $l_c = \nu/u_\tau$, are presented in Fig. 3 and fitted to the above scaling laws over a wide range of Reynolds numbers.

Utilizing the normalized mean velocity distribution, Nikuradse [19] claimed that when data points near the pipe

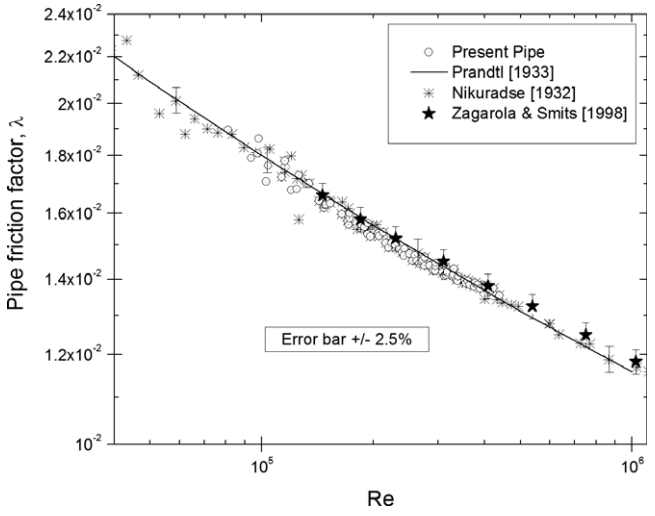

Fig. 2. Present pipe friction factor over an intermediate range of Reynolds numbers compared with literature values.

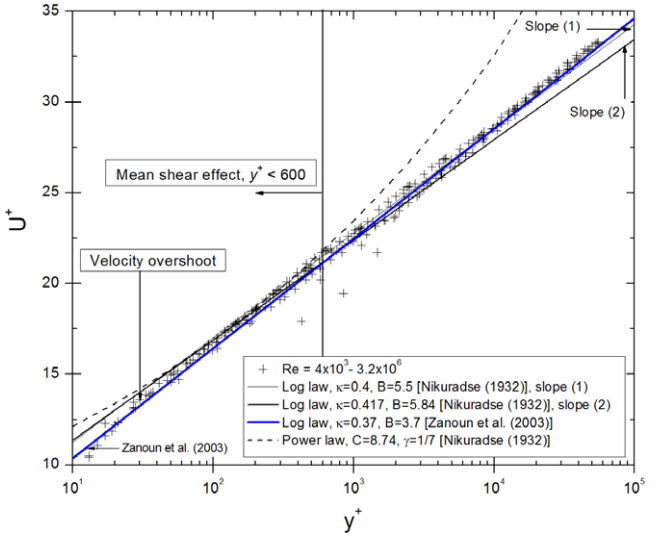

Fig. 3. Representation of the logarithmic velocity profile based on results from Nikuradse [19] in smooth pipe flow over a wide range of Reynolds numbers.

centerline were taken into consideration the logarithmic velocity profile reads as

$$U^+ = 5.75\log(y^+) + 5.5, \tag{16}$$

i.e., $\kappa = 0.4$ and $B = 5.5$ [slope (1) in Fig. 3]. On the other hand, he claimed that when data points near the pipe wall are considered, the logarithmic velocity profile took the following form

$$U^+ = 5.52\log(y^+) + 5.84, \tag{17}$$

i.e., $\kappa = 0.417$ and $B = 5.84$ [slope (2) in Fig. 3].

As a consequence, from Fig. 3 one can see that Nikuradse's analysis for $U^+ = f(y^+)$ to obtain accurate values for the constants of the logarithmic velocity profile seems not to be an appropriate approach. Hence, directly from the mean velocity distribution, i.e., U^+ versus y^+, one cannot obtain the final answer regarding exact values for both the von Kármán constant and the additive constant. For instance, the higher value that Nikuradse recommended, i.e., $\kappa = 0.417$, came out as a result of including his velocity overshoot data for $y^+ \leqslant 600$ into the logarithmic velocity profile, see Fig. 3. On the other hand, by avoiding data under $y^+ = 600$ and considering data points near the pipe centerline he obtained a lower value for the von Kármán constant, i.e., $\kappa = 0.4$.

Moreover, based on the mixing length principle, Nikuradse found a value of 0.38 for velocity data of $Re > 10^5$ which is in very close agreement with values obtained recently by Österlund et al. [22] and Zanoun et al. [34]. The log line of Zanoun et al. [34] was added to Fig. 3 and it was found to represent well the pipe data of Nikuradse even beyond the outer limit (i.e., $y^+ = 0.2\,R^+$) of the log range. It is worth noting that the log line proposed by Zanoun et al. [34] fits Nikuradse's data better than both lines suggested by Nikuradse [19] either with slope (1) or slope (2). Moreover, Nikuradse [19] obtained a value of 0.4 for the von Kármán constant for $Re < 10^5$ also based on the mixing length principle. The different values obtained from the smooth pipe flow data by Nikuradse [19] are ample justifications for the present authors' arguments that new pipe flow data are needed to remedy the unsatisfactory situation with the measured mean velocity distributions.

In spite of the above observation and the occasional claim of inconsistency in Nikuradse's data, the measured velocity profiles of the smooth pipe flow of Nikuradse [19] were analyzed by the present authors with respect to the question of whether the mean velocity profile in the overlap region behaves in a logarithmic or in a power manner, utilizing the diagnostic functions suggested by Österlund et al. [22] and Wosnik et al. [35], i.e., $\Xi = [y^+(\mathrm{d}U^+/\mathrm{d}y^+)]$ and $\Gamma = [(y^+/U^+)(\mathrm{d}U^+/\mathrm{d}y^+)]$, representing the local slope for the log law and the power law, respectively. It is worth noting that the mean velocity gradient was obtained from the normalized mean velocity, U^+, differentiated with respect to the normalized wall distance, y^+, using the three point scheme proposed by Grußman and Roos [13]:

$$\frac{\mathrm{d}U^+}{\mathrm{d}y^+} = \frac{y^+_{i+1} - y^+_i}{y^+_{i+1} - y^+_{i-1}}\,\frac{U^+_i - U^+_{i-1}}{y^+_i - y^+_{i-1}} + \frac{y^+_i - y^+_{i-1}}{y^+_{i+1} - y^+_{i-1}}\,\frac{U^+_{i+1} - U^+_i}{y^+_{i+1} - y^+_i} \tag{18}$$

and Ξ resulted from differentiating Eq. (14), i.e., $\Xi = 1/\kappa = [y^+(\mathrm{d}U^+/\mathrm{d}y^+)]$. Similarly, the function Γ was obtained from differentiating Eq. (15). The outcome of differentiating the mean velocity profiles of Nikuradse [19] is presented in Fig. 4, showing the local distribution of both diagnostic functions, Ξ and Γ, versus the normalized wall distance, y^+. Despite of the wide scatter which can be observed in Fig. 4, it illustrates a constant behavior of Ξ as a function of the normalized wall distance (y^+) for $y^+ > 600$, extending to $y^+ \approx 0.45R^+$, corresponding to the highest value of the Re (i.e., $R^+ = 55400$) achieved by Nikuradse [19], that is beyond the most commonly used outer limit ($y^+ = 0.2\,R^+$) of the log range. The constant behavior of Ξ versus y^+ leads to the existence of a logarithmic layer and supports Millikan's [18] argument that a logarithmic velocity profile is expected in high-Re turbulent pipe flows with a constant value for the von Kármán constant. Therefore, the logarithmic law was taken to be a good representation for the mean velocity of Nikuradse [19] measured in the overlap region of the pipe flow for $R^+ > 4.5 \times 10^3$. On the other hand, the power-law diagnostic function was found to decrease monotonically in the overlap region, and therefore the power law was found to be far from useful for representing the mean velocity profile in the overlap region. However, a constant behavior for the power-law diagnostic function was observed for wall distances $y^+ < 600$ and $y^+ > 10^4$, proposing power layers in the near-wall region and close to the pipe center, respectively.

Further processing of Nikuradse' smooth-pipe mean velocity profiles is presented in Fig. 5 based on a method of data analysis, recently, proposed by Zanoun et al. [34] in the form of $\ln(\mathrm{d}U^+/\mathrm{d}y^+)$ against $\ln(y^+)$. The logarithmic velocity profile was differentiated and arranged to be written as

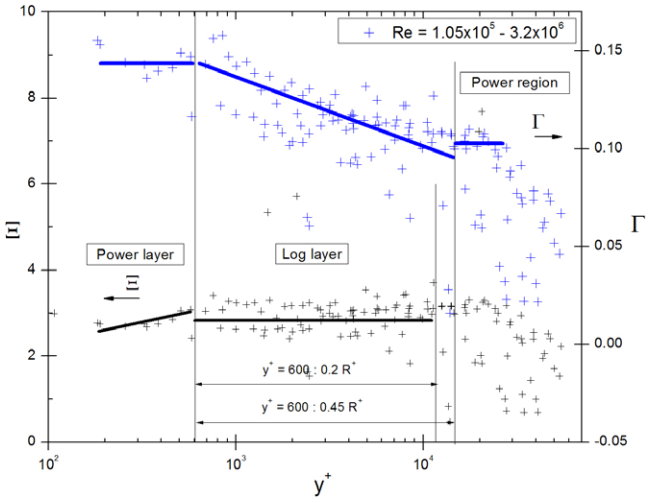

Fig. 4. Distribution of the local diagnostic functions for the mean velocity profiles from Nikuradse [19] in smooth pipe flow experiments.

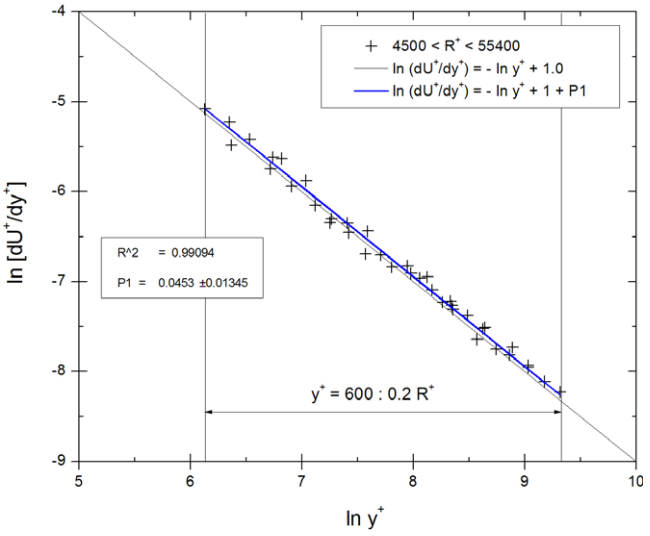

Fig. 5. Ln(dU^+/dy^+) versus ln(y^+) representation of the mean velocity gradient of Nikuradse [19] smooth-pipe data over a wide range of Reynolds numbers using the pitot tube.

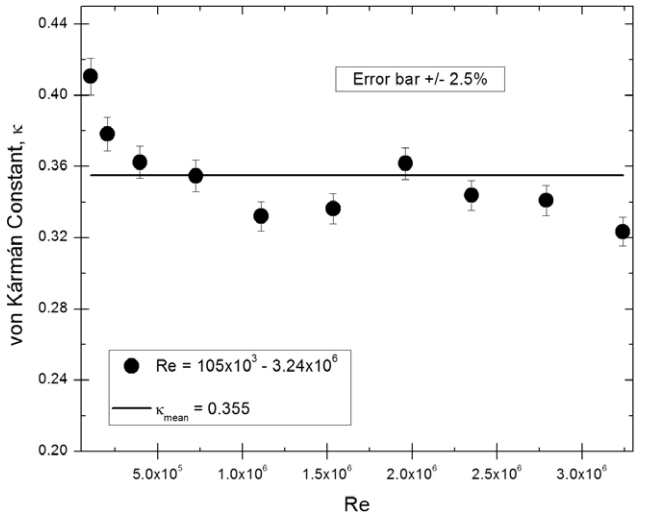

Fig. 6. Summary of the von Kármán constant for the logarithmic velocity profile, based on some individual cases from Nikuradse [19] smooth pipe flow data.

$$U^+ = \frac{1}{\kappa}\ln[y^+] + B \quad \rightarrow \quad \left[\frac{dU^+}{dy^+}\right] = \frac{1}{\kappa y^+} \quad \rightarrow \quad \ln\left[\frac{dU^+}{dy^+}\right] = -\ln[y^+] + \ln\left[\frac{1}{\kappa}\right]. \tag{19}$$

The intercept $\ln[1/\kappa]$ in Eq. (19) was then estimated by fitting Eq. (19) to Nikuradse' smooth-pipe data. The results presented in Fig. 5 are for the log range starting at $y^+ = 600$ as an inner limit, extending to $y^+ = 0.2R^+$ as an outer limit, which is widely used and more convincing for the fluid mechanics community, in spite of the fact that the log layer could be extended to $y^+ = 0.45R^+$ corresponding to the maximum Reynolds number Nikuradse achieved in his experiments, i.e., $R^+ = 55400$, see Fig. 4. The experimental data of Nikuradse plotted in Fig. 5 show a deviation of 4.5% from the line proposed by Zanoun et al. [34]:

$$\ln\left(\frac{dU^+}{dy^+}\right) = -\ln[y^+] + 1. \tag{20}$$

As a result, the value of the von Kármán constant was found to be 0.355, which is lower than the different values obtained by Nikuradse himself, but in good agreement with a value $\kappa = 0.357$ obtained from the analysis of Nikuradse's data presented in Fig. 11 in Hinze's paper (1962) for $Re > 2\times10^5$, and a value $\kappa = 0.36$ obtained by Deissler [9] for the pipe flow. A summary of the values of the von Kármán constant obtained from the analysis of some individual cases of Nikuradse's pipe mean velocity profiles is presented in Fig. 6, resulting in a mean value of $\kappa = 0.355$.

To remedy the unsatisfactory situation with Nikuradse's pitot tube data, the present authors carried out their own pipe flow velocity measurements using two different measuring techniques, namely hot wire anemometry and pitot tube. The outcome of the measurements using the hot wire and a pitot tube of 1 mm inner diameter is presented in Fig. 7, respectively. Comparing Fig. 7a and b, one can conclude that there is an agreement between the general behavior of both diagnostic functions over the different wall layers. For wall distances $y^+ < 300$ a power layer was obtained in both figures since a constant behavior of the power law diagnostic function, Γ, was observed. However, a constant behavior of Ξ was found for the wall interval $300 < y^+ \leqslant 0.2R^+$, suggesting that the logarithmic law describes well the pipe flow data in the overlap region for $R^+ > 4.5\times10^3$. On the other hand, in the core region, the log law was found to be no longer appropriate since a constant behavior was found for the power law diagnostic function.

An observation made by Prandtl [27], Tenneks and Lumley [30], Gad-el-Hak and Bandyopadhyay [12], Zanoun et al. [34], and more recently Kitoh et al. [15] supported the conclusion deduced from Figs. 4 and 7 that the log range could be extended to a wall distance beyond the most accepted outer limit, i.e., $y^+ = 0.2R^+$. Tenneks and Lumley [30] concluded that it so happens that in the pipe flow the velocity profile follows the log law closely up to and somewhat beyond $\eta = r/R = 1/4$ (i.e., $y^+ = 0.25R^+$), even though this is well outside the reach of the inertial sublayer. It was also observed by Zanoun et al. [34] that the interval over which the log law could be applied increases slowly with increasing Reynolds number while the wall interval covered by a Reynolds number-dependent power law decreases with increase in Re. In spite of the fact that the log law could be applied up to $y^+ = 0.25R^+$, the present authors limited their analysis to $y^+ = 0.2R^+$, which is widely used and accepted in the literature for two reasons. The first is that the current pipe data are not for high Reynolds numbers to strongly support extending the log range beyond $y^+ = 0.2R^+$. The second is that researchers in the fluid mechanics community might think that the

Please cite this article in press as: E.-S. Zanoun et al., Wall skin friction and mean velocity profiles of fully developed ..., Exp. Therm. Fluid Sci. (2007), doi:10.1016/j.expthermflusci.2007.04.002

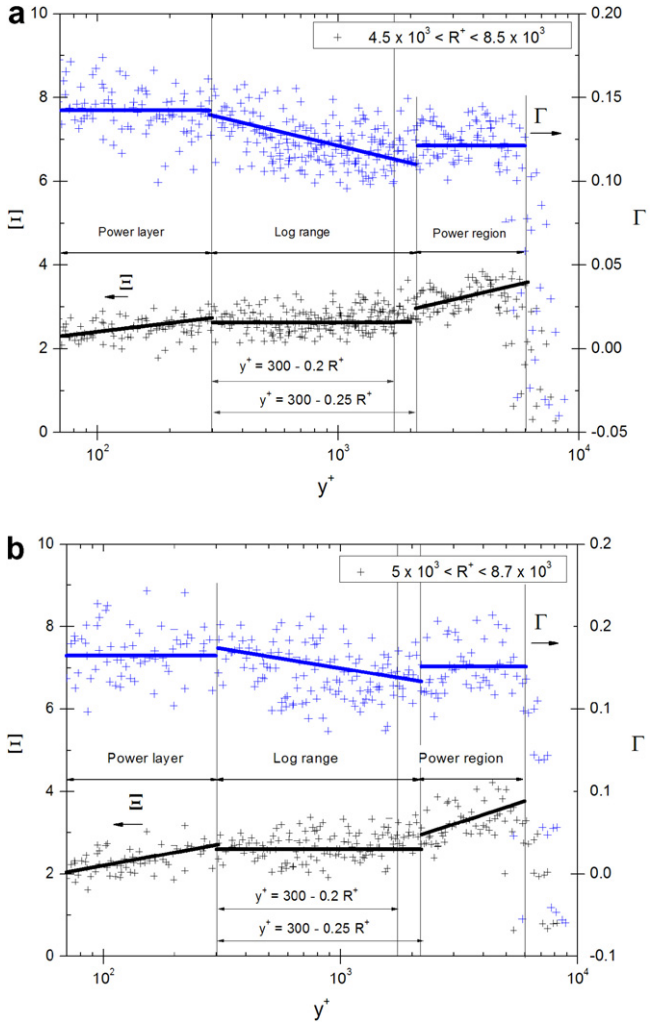

Fig. 7. Diagnostic functions for the mean velocity profiles from the present pipe flow measurements using (a) hot wire and (b) pitot tube.

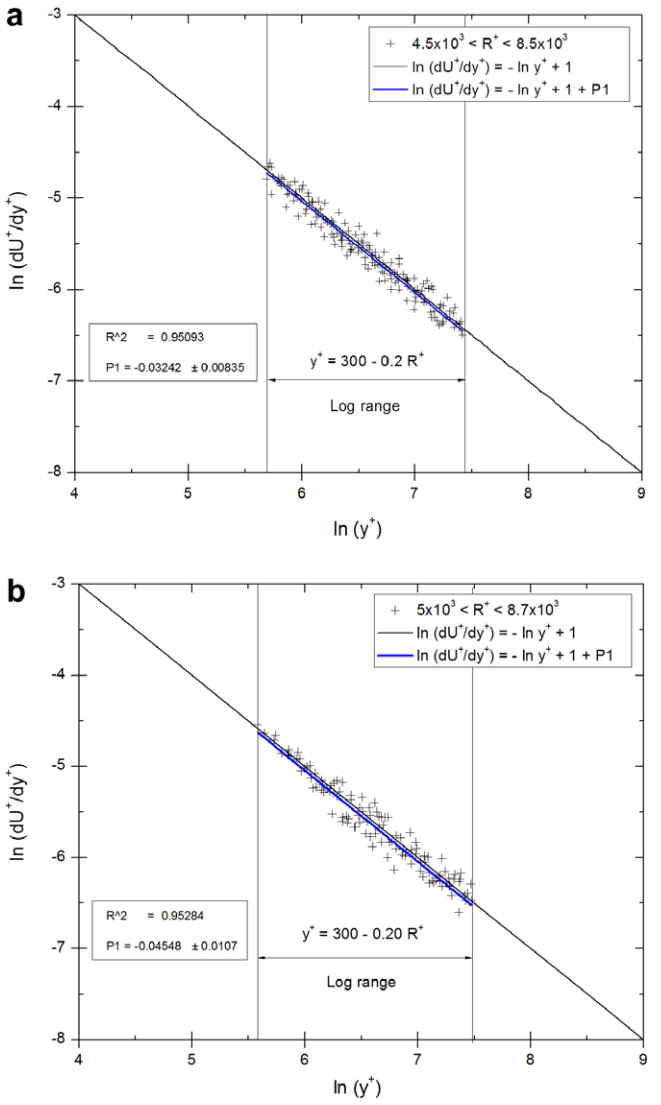

Fig. 8. $\mathrm{Ln}(\mathrm{d}U^+/\mathrm{d}y^+)$ versus $\ln(y^+)$ representation of the mean velocity gradient over a medium range of Reynolds numbers from (a) hot wire and (b) pitot tube measurements.

lower value for the von Kármán constant obtained by the present authors arises because of extending the log range beyond the wall distance $y^+ = 0.2\,R^+$. As a result, the present authors considered the outer limit of the log law to be $0.2\,R^+$. However, a short summary for the effect of the outer limit of the log range on the constants of the logarithmic velocity profile is given in Table 1.

The given values for the constants of the logarithmic velocity profile, i.e., κ and B, summarized in Table 1 were determined based on data presented in Figs. 8 and 9 for the two different log ranges in Table 1 using both the hot wire and the pitot tube measuring techniques. The resultant data led to a logarithmic layer with a value of $\kappa = 0.38$ when using hot wire anemometry and of $\kappa = 0.385$ when pitot tube was utilized for the log range $300 < y^+ \leqslant 0.2\,R^+$. Comparisons of Fig. 8a and b indicates that the slope of the log line deviates approximately 3.24% and 4.55% from the line proposed by Zanoun et al. [34], i.e., Eq. (20), respectively. The small difference between the hot-wire and the pitot tube data indicates that the mean shear effect still slightly influences the pitot tube data even for wall distances $y^+ > 300$, although the pitot tube has a small diameter in terms of wall units.

Similarly, using the least-square curve fit the additive constant (B) of the logarithmic velocity profile was evaluated. The mean value of the additive constant, hence was obtained from the mean velocity profile as described below:

Table 1
Summary of the log law constants for different log ranges of the logarithmic velocity profile from present smooth pipe flow facility

	HWA	Pitot tube	HWA	Pitot tube
Log range (y^+_{iner}–y^+_{outer})	300–$0.15\,R^+$	300–$0.15\,R^+$	300–$0.2\,R^+$	300–$0.2\,R^+$
von Kármán constant, κ	0.384	0.39	0.38	0.385
Additive constant, B	4.43	4.67	4.30	4.45

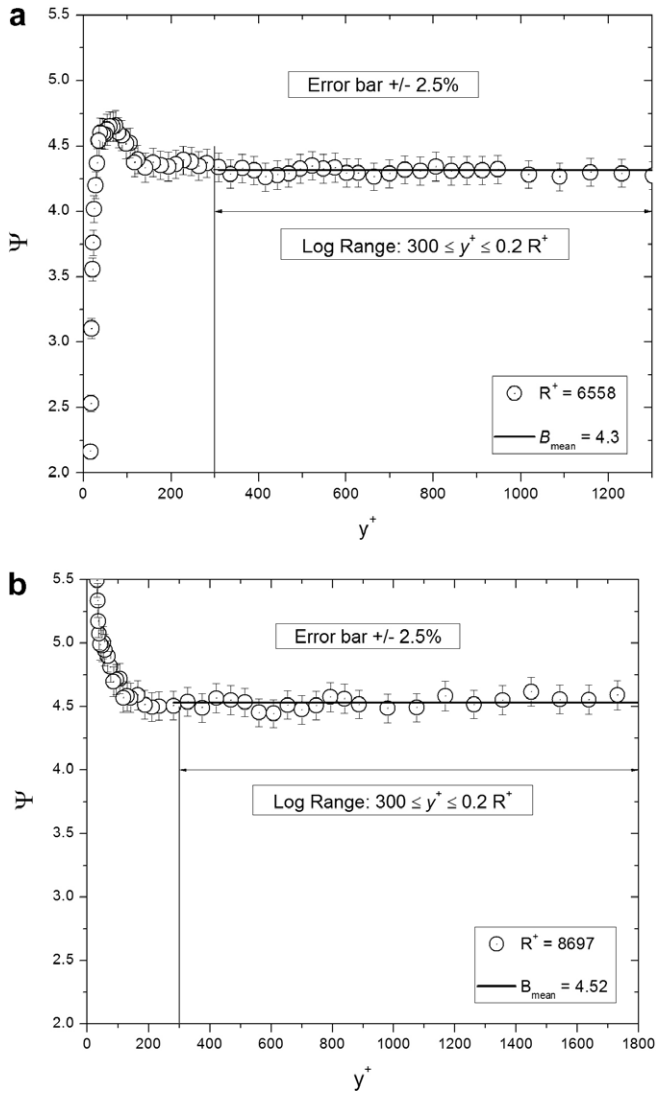

Fig. 9. Present (a) hot-wire and (b) pitot tube additive constant distributions in pipe flow for two different R^+.

$$\Psi = U^+ - \frac{1}{\kappa}\ln y^+. \tag{21}$$

Fig. 9a and b shows the behavior of selected samples of the local function Ψ as defined by Eq. (21) versus the wall distance, y^+, from the hot wire and the pitot tube, respectively. A constant behavior of Ψ was observed in the region where the log law is valid and was considered for an average calculation for the selected two cases as shown in the figure.

In addition to the log layer, two different power layers were observed over the wall distances $y^+ < 300$ and $y^+ > 0.25\,R^+$. The power law constants, i.e., the multiplication factor and the exponent, were found to be:

1. $C = 8.92$ and $\gamma = 0.1355$ for $y^+ < 300$ and $C = 9.5$ and $\gamma = 0.124$ for $y^+ > 0.25\,R^+$,
2. $C = 9.05$ and $\gamma = 0.1324$ for $y^+ < 300$ and $C = 9.5$ and $\gamma = 0.124$ for $y^+ > 0.25\,R^+$for the data obtained from the hot wire and the pitot tube, respectively.

Utilizing the inner scaling variables, the normalized velocity profile data in the pipe flow are presented in Fig. 10a and b. The wall friction velocity, u_τ, used for the normalization was deduced from the mean pressure gradient measurements in the downstream part of the pipe test section where a fully developed flow existed. The mean velocity profiles were then normalized using the corresponding shear velocity to yield $U^+ = U/u_\tau$ and the wall distance with the viscous length scale to give $y^+ = y/l_c$. All the hot-wire velocity profiles are presented in Fig. 10a and compared with the scaling log law:

$$U^+ = \frac{1}{0.38}\ln(y^+) + 4.3 \tag{22}$$

and similarly the pitot tube velocity profiles in Fig. 10b with:

$$U^+ = \frac{1}{0.385}\ln(y^+) + 4.45 \tag{23}$$

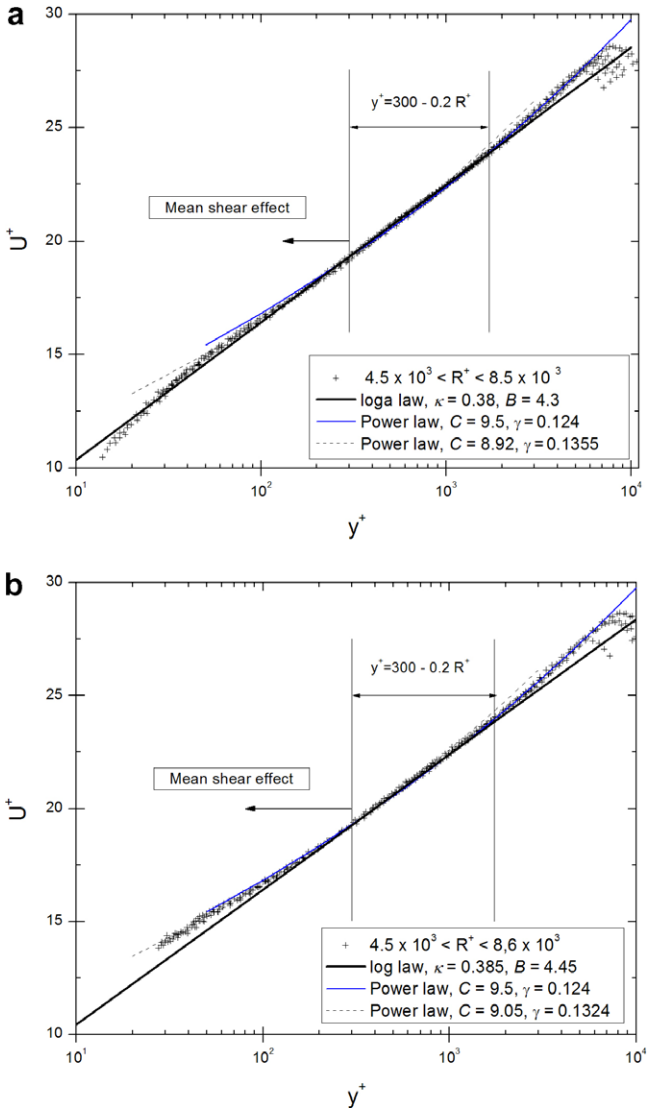

Fig. 10. Present (a) hot-wire and (b) pitot tube mean velocity distributions in pipe flow.

good agreement in both Fig. 10a and b was observed over the wall distance $300 \leqslant y^+ \leqslant 0.2R^+$. Hence, in case of the pipe flow, the log line was found to represent well the pipe data for $R^+ \geqslant 4.5 \times 10^3$. It was also observed that the hot wire and the pitot tube results are about the same and the effect of the mean shear gradient on the pitot probe measurements is minimal if the inner limit of the log range of the logarithmic velocity profile was taken as $y^+ \geqslant 300$. It is worth noting that the values of the log law parameters, i.e., κ and B, used in both Eqs. (22) and (23) are the average values over the present Reynolds number ranges, i.e., $4.5 \times 10^3 < R^+ < 8.5 \times 10^3$, and $5 \times 10^3 < R^+ < 8.7 \times 10^3$, for the hot wire and the pitot tube measurements, respectively.

5. Wall skin friction and log law constants

Further processing of the pipe friction data provides information about the constants of the logarithmic law of the wall. It is worth mentioning that the logarithmic friction relation was deduced by Prandtl [27] based on the assumption that the logarithmic velocity profile is valid from the wall (i.e., $y = 0$) to the centerline of the pipe (i.e., $y = R$). He claimed that the contribution of the difference in mass flux in the near-wall region can be neglected as well as the difference in the core region, at least for $Re \geqslant 10^5$, when predicted using the log law. Hence the general form of the logarithmic friction relation was derived by Prandtl [27] based on complete similarity of the mean velocity profile in both the inner and outer flow regions in the form of Eq. (9), $\sqrt{8/\lambda} = (1/\kappa)\ln(Re\sqrt{\lambda/32}) + B - 3/2\kappa$. However, the deviation of the present mean velocity data in the pipe flow from the log law was observed under $y^+ = 300$ (i.e., velocity overshoot) and also in the core region (i.e., the velocity wake), see Fig. 10a and b, resulting in significant error in the bulk flow velocity (U_b) deduced from Eq. (8) when compared with the actual bulk flow velocity. Consequently, the wall friction factor ($\lambda = 8u_\tau/U_b$) is over estimated when predicted by using Eq. (9) as compared with the direct experimental friction results.

In spite of the incorrect assumptions made to derive the "logarithmic friction relation", there is a claim that it might be used to obtain accurate values for the constants of the logarithmic velocity profile instead of carrying out detailed measurements of the mean velocity distributions, see, e.g., Zagarola and Smits [32]. They claimed that the logarithmic friction relation, i.e., Eq. (9), can be used to determine the von Kármán constant, κ, after rearranging it to take the following simplified form:

$$\sqrt{\frac{1}{\lambda}} = C_1 \log\left(Re\sqrt{\lambda}\right) + C_2, \tag{24}$$

where C_1 and C_2 are coefficients which may or may not be Re dependent. The C_1 and C_2 constants were defined by Zagarola and Smits [32] as follows:

$$C_1 = \frac{1}{2\sqrt{2}\kappa\log(e)},$$
$$C_2 = \frac{B}{2\sqrt{2}} - \frac{1}{\kappa}\left[\frac{\log 4\sqrt{2}}{2\sqrt{2}\log(e)} + \frac{3}{4\sqrt{2}}\right] + C_3 - C_4. \tag{25}$$

They postulated that Eq. (24) can be used to determine κ without the need to evaluate the slope of the mean velocity profile over a limited range of the wall distance. It seems, therefore, at first sight to be an interesting method to estimate κ from some integral flow parameters such as the bulk Reynolds number and the mean pressure gradient. However, Eq. (24) was derived based on wrong assumptions as was clarified and therefore it over estimates the value of the von Kármán constant. As a result, the present authors consider Eq. (24) as unappropriate method as it was claimed to be used to determine an exact value for the slope of the logarithmic velocity profile.

To clarify the above argument, the pipe's friction data of Nikuradse and the present pipe data were analyzed with respect to the question of whether the logarithmic friction relation can be used to derive accurately the constants of the log law or not. Since the pipe data of Nikuradse [19] provided a good basis of pipe's friction data over a wide range of Reynolds numbers, $3 \times 10^3 \leqslant Re \leqslant 3.2 \times 10^6$, the present authors reanalyzed them with respect to Eq. (24). From the analysis of the current pipe data presented in Section 4, the logarithmic velocity profile was found to be superior for $R^+ \geqslant 4500$ (i.e., $Re \geqslant 2 \times 10^5$). Therefore, Nikuradse's friction data were plotted versus the Reynolds number and fitted to Eq. (24) in Fig. 11 for the higher range of Reynolds number data, i.e., $2 \times 10^5 \leqslant Re \leqslant 3.2 \times 10^6$ to determine both C_1 and C_2. The value of the constant C_1 was estimated to be 1.93094, resulting in a value of 0.421 for the von Kármán constant, which is higher than the value obtained by the present authors from the slope of

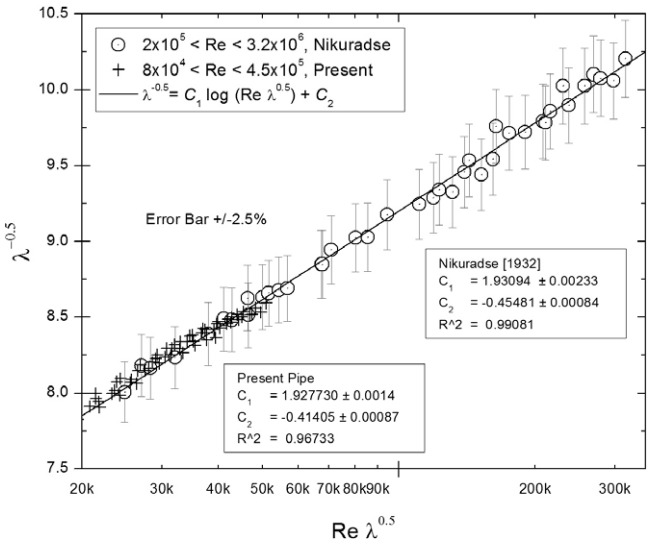

Fig. 11. The present and Nikuradse's pipe friction data fitted to Eq. (24) over a wide range of Reynolds numbers.

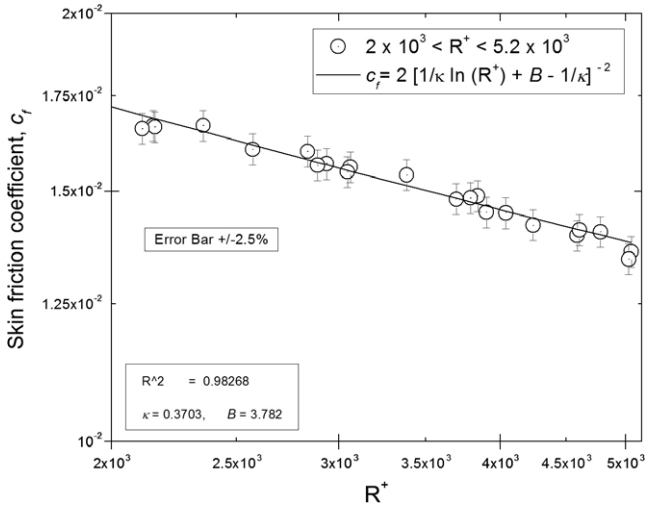

Fig. 12. Consistency check of the log law constants from both skin friction and mean velocity data from channel results of Zanoun et al. [34].

Nikuradse's mean velocity profiles ($\kappa = 0.355$). In a similar way, the present data for $2 \times 10^5 \leqslant Re \leqslant 4.5 \times 10^5$ were also analyzed with respect to Eq. (24), resulting in C_1=1.92773, and therefore κ=0.422 which is in good agreement with the value obtained from Nikuradse's pipe friction data, but it deviates from the value obtained from the slope of the authors' mean velocity profile, i.e., $\kappa = 0.38$.

On the other hand, the deviation of the mean velocity profile from the log law in the near-wall and core regions of the channel flow is much weaker than that for the pipe flow, see Zanoun et al. [34], and therefore their effects for estimating the mass flux are much weaker. This suggests that the log law may be valid much closer to the line of symmetry of the flow in the case of the channel and consequently it is applicable to be used to obtain the logarithmic skin friction relation. This can be verified from Fig. 12, which represents the channel skin friction data of Zanoun et al. [34] used to obtain values for κ and B. An outstanding agreement between the values obtained by Zanoun et al. [34] from the mean velocity profiles, $\kappa = 0.37$ and $B = 3.7$, and values obtained from skin friction data, $\kappa = 0.3703$ and $B = 3.782$, was observed as can be seen in Fig. 12.

6. Conclusions and final remarks

The present work was carried out to re-examine the extensive experimental data of fully developed turbulent smooth pipe flows obtained by Nikuradse [19]. In order to gain an insight into the accuracy of his results, the present authors repeated some of his pitot tube measurements and compared them with corresponding measurements using hot-wire anemometry. The latter provided sufficient spatial resolution in the direction perpendicular to the flow and can therefore be considered best suited to obtain accurate mean velocity measurements and also, to some extent, accurate turbulence information. The friction factor data of Nikuradse agree well with the present authors' skin friction results. On the other hand, the corresponding hot-wire mean velocity profile measurements show differences with Nikuradse's pitot tube measurements. The hot-wire measurements showed that the slope of the logarithmic velocity profile, i.e. the inverse of the von Kármán constant (κ), is inconsistent with the value deduced from the $\lambda(Re)$ measurements performed by the authors as well as by Nikuradse [19]. Nikuradse's pitot tube velocity data yield κ and B constants that are not reflected by their corresponding pressure gradient measurements and when used they led to an over prediction of the wall skin friction by at least 6%. However, it was observed that the hot wire and pitot tube results are about the same and the effect of the mean shear gradient is minimal if the inner limit of the log range of the logarithmic velocity profile is $y^+ \geqslant 300$. Further work, no doubt, for higher Re with high resolution, precise wall-distance measuring technique, and independent wall skin friction data is needed to remedy the unsatisfactory situation found in the literature regarding the pipe shear flow, including the roughness effects.

Acknowledgements

This work received support through the Deutsche Forschungsgemeinschaft, Contract Du101. Without this support the investigations of the present pipe flows would have not been completeted. Osama Saleh received a scholarship from the Egyptian Embassy in Germany and A. Al-Salaymeh a scholarship from the DAAD. Through these scholarships the present work was also sponsored, and this support is gratefully acknowledged. All preliminary work to establish the test facility was financed through internal sources of the Institute of Fluid Mechanics of the FAU Erlangen-Nürnberg.

References

[1] C.J. Abell, Scaling laws for pipe flow turbulence, Ph.D. thesis, University of Mellbourne, Australia, 1974.
[2] J.C. Bhatia, F. Durst, J. Jovanović, Corrections of hot-wire measurements near walls, J. Fluid Mech. 122 (1982) 411.
[3] P.W. Bearman, Corrections for the effect of ambient temperature drift on hot-wire measurements in incompressible flow, Dansk Industri Syndikat Aktieselskab Inf. 11 (1971) 25–30.
[4] J. Boussinesq, Essi sur la théorie des eaux courantes, Mém. Prés. Acad. Si. XXIII, 46, Paris, 1877.
[5] K. Bremhorst, Effect of fluid temperature on hot-wire anemometers and an improved method of temperature compensation and linearization without use of small signal sensitivities, J. Phys. E: Sci. Instrum. 18 (1985) 44–49.
[6] D.W. Bryer, R.C. Pankhurst, Pressure-probe methods for determining wind speed and flow direction, National Physical Laboratory, London, 1971.
[7] F.H. Clauser, The turbulent boundary layer, Adv. Appl. Mech. 4 (1956) 1–51.
[8] G.B. Crowell Jr., H.W. Daniel, D.B. Henery, Comparison of temperature correction methods for hot wire anemometers, Trans. ASME 31 (5) (1988), September–October.

[9] R.G. Deissler, Analysis of turbulent heat transfer, mass transfer and friction in smooth tubes at high Prandtl and Schmidt numbers, NACA Tech. Rep. 12100 (supersedes NACA Tech. Note 3145), 1956.
[10] F. Durst, E.-S. Zanoun, M. Pashtrapanska, In situ calibration of hot wires close to highly heat-conducting walls, Exp. Fluids 31 (2001) 103.
[11] M. Fischer, Turbulente wandgebundene Strömungen bei kleinen Reynoldszahlen, Universität Erlangen Nürnberg, Dissertation, 1999.
[12] M. Gad-el-Hak, P.R. Bandyopadhyay, Reynolds number effect on wall-bounded flows, Appl. Mech. Rev. 47 (1994) 307.
[13] C. Grußmann, H.G. Roos, Numerik der partiellen Differentialgleichungen, B.G. Teubner, Stuttgart, 1994.
[14] J.O. Hinze, Turbulent pipe-flow, Éditions du Centre National de la Researche Scientifique 15, Quai Anatole-France, Paris (VII), 1962.
[15] O. Kitoh, K. Nakabyashi, F. Nishimura, Experimental study on mean velocity and turbulence characteristics of plane Couette flow: low-Reynolds-number effects and large longitudinal vortical structure, J. Fluid Mech. 539 (2005) 199.
[16] J. Laufer, Investigation of turbulent flow in a two-dimensional channel, NACA Report 1053, No. R-1053, Washington, DC, 1951, pp. 1247–1266.
[17] K.I. Loehrke, H.M. Nagib, Experiments on management of free-stream turbulence, AGARD Report No. 598, IIT, Chicago, IL, 1972.
[18] C.M. Millikan, A critical discussion of turbulent flows in channels and circular tubes, in: Proc. 5th Int. Congress of Appl. Mech., 386, 1938.
[19] J. Nikuradse, Gesetzmässigkeiten der turbulenten Strömung in glatten Rohren, Forschg. Arb. Ing.-Wes. 356 (1932).
[20] J. Nikuradse, Strömungsgesetze in rauhen Rohren, Forschg. Arb. Ing.-Wes. 361 (1933).
[21] J.M. Österlund, A.V. Johansson, H.M. Nagib, M.H. Hites, Wall shear stress measurements in high Reynolds number boundary layers from two facilities, AIAA Paper 99-3814, 30th Fluid Dynamics Conference, Norfolk, VA, 1999.
[22] J.M. Österlund, A.V. Johansson, H.M. Nagib, M.H. Hites, A note on the overlap region in turbulent boundary layers, Phys. Fluids 12 (2000) 1.
[23] R.L. Panton, A Reynolds stress function for wall layers, J. Fluids Eng. 119 (1997) 325–330.
[24] V.C. Patel, M.R. Head, Some observations on skin friction and velocity profiles in fully developed pipe and channel flows, J. Fluid Mech. 25 (1974) 181.
[25] L. Prandtl, Uber die ausgebildete Turbulenz, Z. Angew. Math. Mech. 5 (1925) 136.
[26] L. Prandtl, Zur turbulenten Strömung in Rohren und längs Platten, Ergeb. Aerodyn. Versuch. Göttingen IV. Lieferung, 18, 1932.
[27] L. Prandtl, Reibungswiederstand, hydrodynamische Probleme des Schiffsantriebs, herausgeg, v. G. Kempf u. E. Förster 1932 S. 87; – Neuere Ergebnisse der Turbulenzforschung, Z. VDI Bd. 77 (1933) Nr. 5 S. 105; – Ergebnisse der Aerodynamischen Versuchsanstalt Göttingen, 3 Lief. (1927) S. 1, (English Transl. NACA TM 720).
[28] S. Sami, The pitot tube in turbulent shear flow, in: Proc. 11th Midwestern Mech. Conf., Dev. in Mechanics, vol. 5, Paper 11, 1967, p. 171.
[29] G.I. Taylor, The transport of vorticity and heat through fluid in turbulent motion, Proc. Roy. Soc. London 135 (1932) 685.
[30] H. Tenneks, J.L. Lumley, A first course in turbulence, The MIT Press, 1972.
[31] Th von Kármán, Mechanische Ähnlichkeit und Turbulenz, Nachr. Ges. Wiss. Göttingen, Math. Phys. Klasse 58 (1930).
[32] M.V. Zagarola, A.J. Smits, Mean-flow scaling of turbulent flow, J. Fluid Mech. 373 (1998) 33.
[33] E.-S. Zanoun, H. Nagib, F. Durst, P. Monkewitz, Higher Reynolds number channel data and their comparison to recent asymptotic theory, in: Proc. of 40th AIAA-1102, Aerospace Sciences Meeting, Reno, NY 2002.
[34] E.-S. Zanoun, F. Durst, H. Nagib, Evaluating the law of the wall in two-dimensional fully developed turbulent channel flows, Phys. Fluids 10 (2003) 1–11.
[35] M. Wosnik, L. Castillo, W. George, A theory for turbulent pipe and channel flows, J. Fluid Mech. 421 (2000) 115.

Please cite this article in press as: E.-S. Zanoun et al., Wall skin friction and mean velocity profiles of fully developed ..., Exp. Therm. Fluid Sci. (2007), doi:10.1016/j.expthermflusci.2007.04.002